Spin exchange in polarized deuterium

B. von Przewoski,[1] H. O. Meyer,[1] J. Balewski,[1] W. W. Daehnick,[2] J. Doskow,[1] W. Haeberli,[3] R. Ibald,[1] B. Lorentz,[4] P. V. Pancella,[5] R. E. Pollock,[1] F. Rathmann,[4] T. Rinckel,[1] Swapan K. Saha,[6,2] B. Schwartz,[3] P. Thörngren-Engblom,[7] A. Wellinghausen,[1] T. J. Whitaker,[1] and T. Wise[3]

[1]*Indiana University Cyclotron Facility, Milo B. Sampson Lane, Bloomington, Indiana 47405, USA*

[2]*University of Pittsburgh, Pittsburgh, Pennsylvania 15260, USA*

[3]*University of Wisconsin, Madison, Wisconsin 53706, USA*

[4]*Forschungszentrum Jülich, Jülich, Germany*

[5]*Western Michigan University, Kalamazoo, Michigan 49008, USA*

[6]*Bose Institute, Calcutta 700009, India*

[7]*Uppsala University, Uppsala, Sweden*

(Received 14 February 2003; published 10 October 2003)

We have measured the vector and tensor polarization of an atomic deuterium target as a function of the target density. The polarized deuterium was produced in an atomic beam source and injected into a storage cell. For this experiment, the atomic beam source was operated without rf transitions, in order to avoid complications from the unknown efficiency of these transitions. In this mode, the atomic beam is vector and tensor polarized and both polarizations can be measured simultaneously. We used a 1.2-cm-diam and 27-cm-long storage cell, which yielded an average target density between 3 and 9×10^{11} at/cm^3. We find that the tensor polarization decreases with increasing target density while the vector polarization remains constant. The data are in quantitative agreement with the calculated effect of spin exchange between deuterium atoms at low field.

DOI: 10.1103/PhysRevA.68.042705 PACS number(s): 34.50.−s, 39.10.+j, 29.25.Pj, 24.70.+s

I. INTRODUCTION

When two atoms with antiparallel electron spins collide, both spins flip with a large probability while conserving the longitudinal component of the total spin angular momentum. Due to this effect, the populations of the hyperfine states tend towards equilibrium, the so-called spin-temperature distribution. The rate at which the equilibrium is approached depends on the collision rate.

It is known that spin-exchange collisions may affect the polarization of polarized gas targets. For instance, laser-driven deuterium targets rely on spin-exchange collisions of optically pumped, polarized potassium atoms with deuterium atoms and subsequent spin-exchange collisions between deuterium atoms [1]. The spin-exchange rate is proportional to the number density of the atoms.

If an atomic beam source is used to inject a storage cell target with polarized atoms, spin-exchange effects are usually thought to be unimportant since such a target is much less dense than an optically pumped target. However, even in this case, significant depolarization occurs for tensor-polarized deuterons, as we will demonstrate in this paper. Our study has been prompted by a departure of the tensor polarization of the PINTEX (polarized internal target experiments) polarized deuterium target [2] from the value expected without spin exchange.

There exists one previous observation of spin-exchange effects in a deuterium target [3], where measured changes of the tensor polarization as a function of the magnetic field at the target are found to be in qualitative agreement with the theoretical expectation [4] (for a comparison with the present experiment, see Sec. VI).

II. EXPERIMENTAL SETUP

The experiment was performed at the Indiana Cooler with a stored, unpolarized, 135-MeV proton beam. A layout of the experiment is shown in Fig. 1. Polarized deuterons are produced in an atomic beam source (ABS) [5]. The atoms emerge from the dissociator (a) through an aluminum nozzle, which is cooled to liquid nitrogen temperature. The atomic beam passes along the axis of a set of sextupole magnets (b), which defocus one of the two electron-spin substates. The remaining beam contains deuterium atoms in hyperfine states 1, 2, and 3 (it is customary to number the states in decreasing

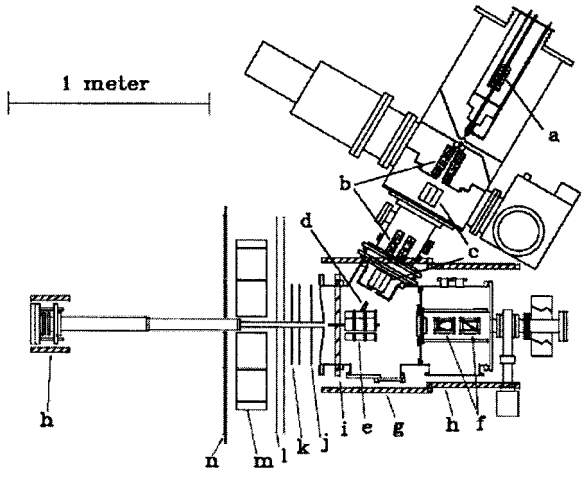

FIG. 1. The PINTEX facility at the Indiana Cooler. *a*, dissociator; *b*, sextupole system; *c*, remotely controlled transition units; *d*, feedtube and target cell; *e*, silicon barrel; *f*, beam position monitors; *g*, Helmholtz coils; *h*, compensating coils; *i*, *z*-field coil; *j*, ΔE scintillator; *k*,*l*, wire chambers; *m*, stopping scintillator; *n*, veto scintillator. The beam direction is from right to left.

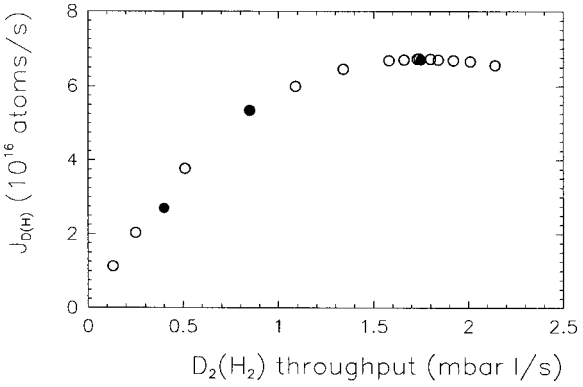

FIG. 2. Atomic beam current into a 1-cm-diam opening vs the flow rate of $D_2(H_2)$ gas into the dissociator. The open circles are from Ref. [5]. The solid dots represent the measured luminosity during this experiment, multiplied by an arbitrary factor.

order of their energy in a magnetic field; for more detail, see, e.g., Ref. [6]). When the states 1, 2, and 3 are equally populated, and the ambient field is ''weak'' (i.e., does not decouple the electron from the nucleus), the nuclear vector polarization P_z equals $+\frac{1}{3}$ and the tensor polarization P_{zz} equals $-\frac{1}{3}$. In reality, the polarization is lower because the spin state separation by the sextupoles is not perfect: a molecular component may be present and wall collisions lead to some depolarization. Larger polarization can be achieved by inducing transitions between substates. In this experiment, however, such rf transitions were not used in order to avoid an assumption about their efficiency.

The internal target consists of a storage cell, located in a weak holding field of 0.3 mT, generated by a set of Helmholtz coils (*i*,*g*). In a storage ring, a weak field is preferred because it avoids significant orbit distortions. The atomic beam enters the storage cell through a 13.0-cm-long, 1.1-cm-diam feed tube (*d*). The target cell is a 27-cm-long tube of 1.2-cm diam made from 0.05-mm-thick aluminum, coated with Teflon in order to minimize depolarization by wall collisions [7]. The length of the cell between the feed tube and the downstream end is 12.5 cm; the upstream part is 14.5 cm long. The sum of the conductances of the three legs for atomic deuterium at 300 K is 15.0 l/s [calculated by using Eq. (1) of Ref. [8]]. The atomic beam current J (at/s) divided by the conductance equals the target density in the center of the cell. The average target density is half this value.

The atomic beam current depends on the flow rate of D_2 gas into the dissociator. This is demonstrated by the open symbols in Fig. 2, which show a measurement [5] of the current J as a function of the gas input when the source is operated with hydrogen. Normally, the gas flow is chosen such that J is optimized. However, in order to vary the density of the target, we operated the ABS at ''normal'' gas flow, as well as at half and at a quarter of the normal gas flow. The solid symbols in Fig. 2 show the relative target thickness during this experiment, obtained by dividing the event rate by the stored proton current. After arbitrary normalization, these data obviously confirm the dependence of J on the gas flow into the dissociator.

While thus the *relative* atomic beam current J for the three flow rates is well known, its absolute value is not accurately known. Experience shows that routine operation corresponds to about $\frac{2}{3}$ of the peak performance shown in Fig. 2. In addition, replacing H_2 by D_2 in the dissociator is known to reduce the flux by roughly a factor of 0.7. Altogether, this leads to a scaling factor of $f_J=0.46$ for the current J in Fig. 2. Since this figure is based on a rough estimate, we explore in Sec. V the dependence of our conclusions on the scaling f_J. It turns out that the most likely value ($f_J=0.38$) is somewhat smaller than the above estimate (see Sec. V). Thus, the currents corresponding to the three flow rates are $J=(2.6,2.0,1.1)\times10^{16}$ at/s, respectively, and the average number density of atoms in the cell is $n_D=(8.5,6.6,3.6)\times10^{11}$ cm^{-3}.

The outgoing proton and deuteron from *pd* elastic scattering are detected in coincidence. The forward going particle (either *p* or *d*) is detected in a stack consisting of a ΔE scintillator (*j*), two wire chambers (*k*,*l*), and a stopping scintillator (*m*) [9]. Laboratory polar angles from 10° to 45° are covered. The recoil particle is detected in the so-called silicon barrel (*e*), an array of 18 silicon strip detectors surrounding the target cell. The strips are oriented in such a way that they measure the azimuth of the recoil, enabling us to impose a coplanarity condition on the two outgoing particles, in order to reject break-up events. Elastic scattering events are further selected by particle identification via $\Delta E-E$ in the forward detector, and by the correlation between energy and angle of the forward particle and between forward scattering angle and recoil pulse height in the silicon detector.

During a given measurement, the holding field, and thus the direction of the spin alignment axis, is cycled between horizontal, vertical, and longitudinal and from positive to negative in 2 s intervals. When the field is reversed, the vector polarization reverses sign, whereas the tensor polarization does not.

III. MEASUREMENT AND ANALYSIS

For the three target densities mentioned in the previous section, the vector and tensor polarization of the target are measured simultaneously as follows.

To evaluate the elastic scattering yields, laboratory polar angles θ from 19° to 33° are accepted. The cross section with a polarized target depends on the azimuth φ of the scattering plane. In the case of a vertical spin alignment axis, for instance, vector moment it_{11} of the polarization induces a term that is proportional to $\cos\varphi$, while the tensor moment t_{22} contributes a $\cos2\varphi$ term. The angle φ is measured by the wire chambers. The accepted φ range is divided into four sections centered about 0°, 180°, 90°, and 270°, corresponding to left, right, up, and down, respectively. The limits for the four sections are set to $\pm44°$ about the center values when evaluating the vector polarization, and $\pm22°$ in the case of tensor polarization. The vector polarization is determined from the left/right and up/down asymmetries for the vertical and horizontal holding field, respectively. The tensor polarization is determined from the sum of the up and down yields and the sum of the left and right yields. The effective analyzing powers iT_{11} and T_{22} are deduced from the known

vector and tensor analyzing powers in *pd* elastic scattering at 135 MeV [10], averaged over the respective θ and φ acceptances. The average is weighted with the θ and φ dependence of the total yield, which represents the detector efficiency.

Varying the φ integration limits changes the effective analyzing powers, but not the resulting polarizations. Variations in the acceptance criteria for an elastic event have no significant effect on the measured polarizations. This demonstrates that a possible background contamination can be discounted.

IV. COMPARISON WITH THEORY

Walker and Anderson [4] predict the loss of polarization of a deuterium target due to spin-exchange collisions by calculating—starting from a given initial state—the evolution of the population of the substates in terms of the parameter t/T_{D}, where t is the average dwell time of an atom in the target and $1/T_{\mathrm{D}}$ is the DD spin exchange rate. The average dwell time is estimated from $t=N_c(d/v)$, where N_c is the average number of collisions with the cell walls, d is the average distance traveled between collisions, and v is the average velocity. A Monte Carlo tracking calculation leads to $N_c \approx 200$ for our cell geometry [8]. Assuming that the probability of emission after a wall collision follows Lambert's cosine law of ideal diffuse reflection, one can calculate geometrically the average distance d to the next collision. For an infinitely long cylinder, one finds that d equals the diameter of the cylinder. The finite-length correction for our target cell is less than 1%. Thus, we set $d=1.2$ cm.

The spin-exchange rate $1/T_{\mathrm{D}}$ is the product of the spin-exchange cross section, $\sigma_{\mathrm{SE}}(\mathrm{DD})=2\times10^{-15}$ cm^2 [4], the number density of atoms n_{D}, and the velocity v of the atoms. The spin-exchange cross section is not expected to significantly depend on either the velocity or the magnetic field, nor has there ever been any experimental evidence of such a dependence. We therefore take its value as a constant, $\sigma_{\mathrm{SE}}(\mathrm{DD})=2\times10^{-15}$ cm^2 [4]. The parameter t/T_{D} that is relevant for a spin-exchange calculation is then proportional to the number density, independent of the velocity, and is given by

$$t/T_{\mathrm{D}}=\sigma_{\mathrm{SE}}(\mathrm{DD})n_{\mathrm{D}}N_c d\zeta_B. \tag{1}$$

The factor ζ_B takes into account the slowing down of the relaxation rate at magnetic fields large enough to decouple the electron and nuclear spins. For vanishing external magnetic field, $\zeta_B=1$. From Eq. (1) in Ref. [4] one obtains $\zeta_B=\{1+[g_S\mu_B(B/\delta_v)]^2\}^{-1}$, where $g_S=2.002$ is the electron g factor, $\mu_B=5.79\times10^{-11}$ MeV/T is the Bohr magneton, and $\delta_v=1.66\times10^{-13}$ MeV is the hyperfine splitting for the deuteron. With these values, we find that our guide field of 0.3 mT hardly affects the spin-exchange rate ($\zeta_B=0.96$).

Assuming that the density n_{D} in Eq. (1) can be replaced by the average over the length of the target cell, we evaluate t/T_{D} for the three target densities mentioned earlier (see Sec. II). Figure 3 shows the measured vector polarization P_z and negative tensor polarization $-P_{zz}$ as a function of t/T_{D}.

Walker and Anderson calculated the evolution of the six substrates in a vanishing field for the case where initially the states 1, 2, and 3 are equally populated while the other three are empty (see Fig. 6 of Ref. [4]). Using the known vector and tensor polarization of individual substates in a weak field [6], the evolution of P_z and P_{zz} can then be easily calculated. The result is shown as dotted lines in Fig. 3. As can be seen, the vector polarization is hardly affected by spin exchange (it actually increases slightly with density).

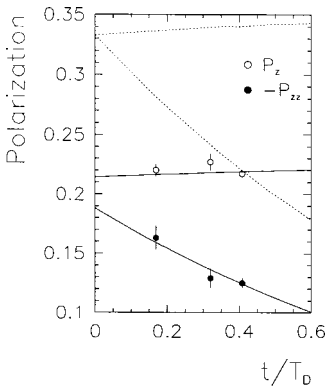

FIG. 3. Vector polarization (open circles) and tensor polarization (solid dots) as a function of t/T_{D} (proportional to the target density). The dotted curves are the predictions by theory [4]. The solid curves are the same, scaled to best fit the data.

The solid lines are the predictions each normalized by an arbitrary factor such that the χ^2 between the data and the calculation is minimized. The normalization factors (0.56 for the tensor polarization and 0.64 for the vector polarization) are discussed in the next section. It can be seen from Fig. 3 that the expected dependence on t/T_{D} (or target density) of both vector and tensor polarization is consistent with the data.

V. DEPENDENCE OF THE RESULT ON TARGET DENSITY

In Fig. 3, the predictions for the vector and tensor analyzing powers have been individually normalized to fit the data. The normalization accounts for the loss of polarization due to wall collisions, recombination, and incomplete rejection of unwanted states in the sextupoles. Earlier we saw that the number density n_{D} of atoms in the cell depends on the factor f_J used to normalize the ordinate of Fig. 2. According to Eq. (1), the ordinate of Fig. 3, t/T_{D}, scales with the same parameter. Since the vector analyzing power is practically independent of t/T_{D}, the normalization factor for the vector polarization, $r_z=0.643\pm0.007$, is unaffected by a change in f_J. However, this is not the case for the best-fit normalization r_{zz} of the tensor polarization. Figure 4(a) shows r_{zz} for five assumed values of f_J. Figure 4(b) shows the χ^2 per degree of freedom of the data relative to the normalized calculations for the same five values of f_J, indicating a preference for $f_J=0.38$, corresponding to $r_{zz}=0.56$. We thus find that the best-fit normalizations r_z and r_{zz} are significantly different from each other, or that the loss of polarization with respect to the ideal value is different for vector and tensor polarization. That this finding is indeed expected can be understood with a simple model for depolarization.

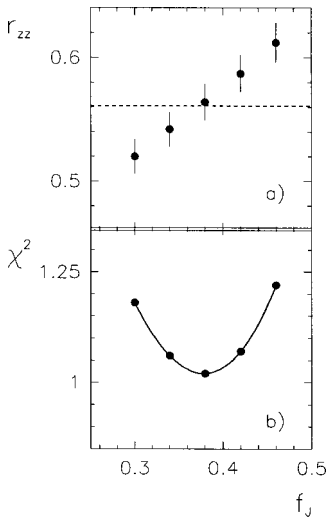

FIG. 4. (a) Dependence of the best-fit normalization r_{zz} of the tensor polarization as a function of f_J. The dashed line indicates the prediction of a simple model for depolarization (see text). (b) χ^2 per degree of freedom of the data relative to the normalized calculations as a function of f_J, indicating a preference for $f_J = 0.38$.

Assume that the depolarizing mechanism is the exchange of the atomic electron with one of random orientation (e.g., during a wall collision). This means that either nothing happens or that the electron spin is flipped. In the latter case, the atom makes a transition, for instance from state 1 to state 6 (or $2 \rightarrow 5$ or $3 \rightarrow 4$, or vice versa). Thus the initial-state occupations evolve. The final polarization depends on the initial state, the number of electron spin flips, and the magnetic field. It is easy to see that the evolution is not the same for vector and tensor polarization. For equal initial population of states 1, 2, and 3, for a weak field, and for a number of electron spin flips that would lower the vector polarization by a factor of 0.643 (our observed value for r_z), one finds that, at the same time, the tensor polarization would have decreased by 0.561. This value is shown as a dashed line in Fig. 4(a). To be sure, the depolarization mechanism postulated here is speculative, and we assume that all polarization loss is by this mechanism, however it is remarkable that the same density normalization f_J that yields a minimum in χ^2 also supports the relative vector-tensor depolarization predicted by our simple model.

VI. CONCLUSION

We have measured the vector and tensor polarization of a polarized deuterium target in a weak magnetic field as a function of target density. The measured polarizations agree well with a model calculation taking into account spin exchange between deuterium atoms. This demonstrates that even for densities below 10^{12} cm^{-3}, depolarization by spin exchange may be sizeable.

In comparison to an earlier study of the change in tensor polarization as a function of the magnetic field at the target [3], the present evidence is based on a direct measurement of the target polarization via the known *pd* scattering analyzing powers, without assumptions about the efficiency of the transition units. The simultaneous measurement of vector and tensor polarization also confirms the predicted relative effect of spin exchange where only the tensor polarization is affected significantly.

ACKNOWLEDGMENTS

The work has been supported by the National Science Foundation and by the U.S. Department of Energy under NSF Grant Nos. PHY-9602872, PHY-9722556, PHY-9901529, and DOE Grant No. DOE-FG02-88ER40438. We are grateful to the IUCF operators for their untiring efforts to deliver stable beam to the experiment.

[1] K. P. Coulter, R. J. Holt, E. R. Kinney, R. S. Kowalczyk, D. H. Potterveld, L. Young, B. Zeidman, A. Zghiche, and D. K. Toporkov, Phys. Rev. Lett. **68**, 174 (1992).
[2] https://ceem.indiana.edu/PINTEX/index.html
[3] H. J. Bulten, Z.-L. Zhou, J. F. J. van den Brandt, M. Ferro-Luzzi, and J. Lang, Phys. Rev. A **58**, 1146 (1998).
[4] T. Walker and L. W. Anderson, Nucl. Instrum. Methods Phys. Res. A **334**, 313 (1993).
[5] T. Wise, A. D. Roberts, and W. Haeberli, Nucl. Instrum. Methods Phys. Res. A **336**, 410 (1993).
[6] W. Haeberli, Annu. Rev. Nucl. Sci. **17**, 373 (1967).
[7] J. S. Price and W. Haeberli, Nucl. Instrum. Methods Phys. Res. A **349**, 321 (1994).
[8] K. Zapfe, W. Brückner, H.-G. Gaul, M. Grieser, M. T. Lin, Z. Moroz, B. Povh, M. Rall, B. Stechert, E. Steffens, J. Stenger, F. Stock, J. Tonhäuser, Ch. Montag, F. Rathmann, D. Fick, B. Braun, G. Graw, and W. Haeberli, Nucl. Instrum. Methods Phys. Res. A **368**, 293 (1996).
[9] T. Rinckel, P. Thörngren-Engblom, H. O. Meyer, J. T. Balewski, J. Doskow, R. E. Pollock, B. von Przewoski, F. Sperisen, W. W. Daehnick, R. W. Flammang, Swapan K. Saha, W. Haeberli, B. Lorentz, F. Rathmann, B. Schwartz, T. Wise, and P. V. Pancella, Nucl. Instrum. Methods Phys. Res. A **439**, 117 (2000).
[10] K. Sekiguchi, H. Sakai, H. Witala, W. Glöckle, J. Golak, M. Hatano, H. Kamada, H. Kato, Y. Maeda, J. Nishikawa, A. Nogga, T. Ohnishi, H. Okamura, N. Sakamoto, S. Sakoda, Y. Satou, K. Suda, A. Tamii, T. Uesaka, T. Wakasa, and K. Yako, Phys. Rev. C **65**, 034003 (2002).